

Due to a lot of requests, we are making the complete data sets from our paper available for download. We have included some of our unpublished analysis as well. If you decide to use these materials for your work, we ask to acknowledge/cite the source. – S. J.

I. Explanation of the data.

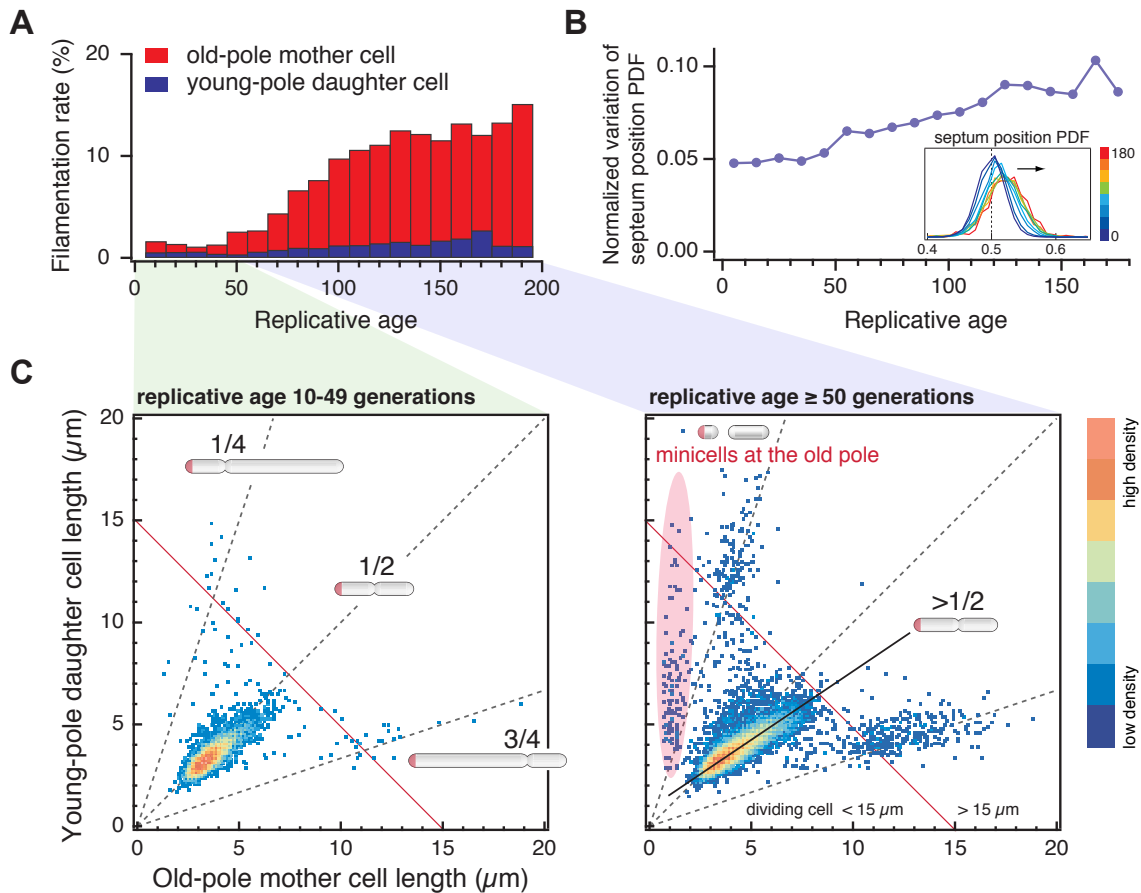
We used four strains: SJ108 and SJ119 (*E. coli* B/r), *E. coli* MG1655 (CGSC 6300) and MG1655 *lexA3* [See, Wang *et al.*, Curr Biol 20, 1099-1103 (2010)]. For each experiment, we followed multiple fields of view (xy01, xy02, xy03...); each field of view consists of multiple channels (ch0, ch1, ch1...); in each channel, we followed at least four left-most cells in the lineage tree: cell0 = the old-pole mother cell, cell1 = the young-pole daughter cell, cell2 & cell 3 = the two daughters of cell1. See Supplementary Experimental Procedures in our paper, and you will see what we mean very clearly.

Each data file (.dat) contains 8 columns:

1. time: lab time in minutes
2. division: 1 = the cell is dividing, 0 = the cell is not dividing
3. length: cell length in pixels (1 pixel = 0.0645 μm)
4. width: cell width in pixels
5. area: projected area of the cell in pixels
6. Intensity: average YFP intensity of the cell (arbitrary unit)
7. CMx: x coordinate of the center of mass of the cell (in pixels)
8. CMy: y coordinate of the center of mass of the cell (in pixels)

Important: virtually every image analysis method relies on some kind of thresholding. Thresholding is fine as long as it is applied equally and consistently to the images. In our case, however, each growth channel in the mother machine has one open-end and one closed-end. Thus, the optical properties of the microfluidic growth channel show spatial variations at its closed-end. What this means is that we had to use two different thresholds for segmentation of the cells: one for the old-pole of cell0 at the closed-end of the channel, and the other for the rest. This is important to remember because the measured cell length of cell0 could be systematically different from cell1 (cell2, cell3, ...) by one or two pixels. And 1-2 pixel difference translates into about 1%-2% systematic differences in growth rates between cell0 and cell1. In general, it is extremely important to understand in detail how the experiment and analysis were done (especially if you are a theoretician who are trying to model the data).

II. A closer look at the data

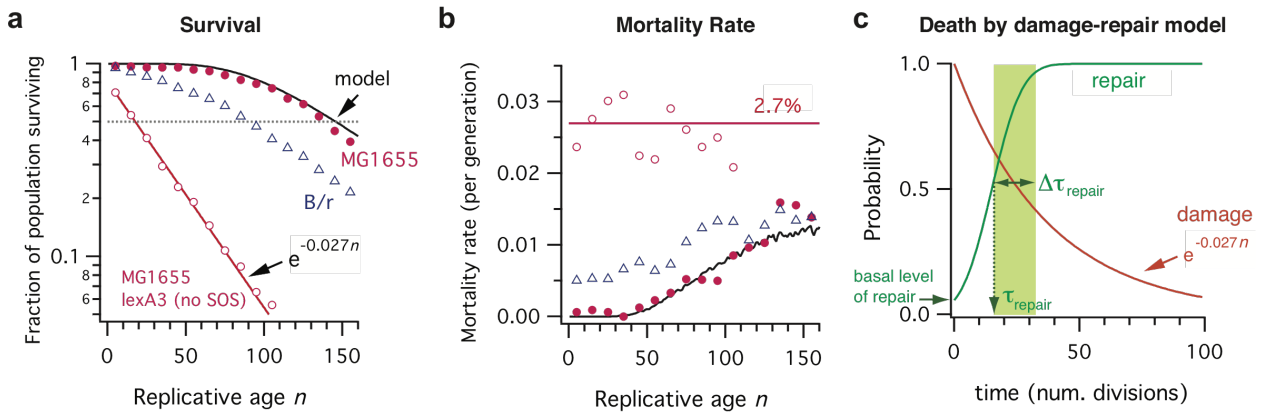


There is a lot of information to be unveiled from the data. To give an example, Panel A is a result we published, which shows increasing filamentation rate of the old-pole mother cell after the first 50 generations. A closer look at the data reveals striking differences in division patterns between the mother cells (cell0) and the daughter cells (cell1). For instance, Panel B shows a normalized variation (= coefficient of variation) of the septum position probability distribution function (PDF) vs. replicative age of the cell. Clearly, the old-pole mother cell gradually loses her ability to precisely determine the mid-cell position starting after the first ~50 divisions.

How about looking at cell0 vs. cell1? Panel C shows that. The diagonal line represents a perfect symmetry of cell division, namely, division at the midcell. With time, the size of the mother cell increases relative to the daughter cell. Filaments longer than $15 \mu\text{m}$ never divide at the midcell but at the quarter positions, in good agreement with a fixed $8 \mu\text{m}$ wavelength of Min-protein oscillations [D. M. Raskin

and P. A. J. de Boer, PNAS 96, 4971– 4976 (1999).] Surprisingly, after the first 50 generations, minicells are formed exclusively at the old pole. *E. coli* mutants, lacking the *min* CDE genes, whose products determine the location of the septum, have similar defects in septal positioning that result in production of a mixture of filaments and minicells [H. I. Alder, W. D. Fisher, A. Cohen, A. A. Hardigree, PNAS 57, 321-326 (1967)]. We have several hypotheses for the division patterns, and our favorite is that the physically aging cell wall at the old pole has increasing defects due to its “metabolic inertness” [A.L. Koch and C.L. Woldringh. The metabolic inertness of the pole wall of a Gram-negative rod. J. theor. Biol. 171: 415-425 (1994)]. The metabolically inert aging cell wall could attract a lethal element. It remains to be understood if and how the lethal element can trigger filamentation and lead to cell death. One possibility is that the aberrant cell division that is observed could lead to extensive DNA damage resulting in cell death.

III. Accumulating damage and repair model of aging. Another interesting observation of our data is the increasing mortality rate of the *E. coli* cells, in stark contrast to the constant elongation rate of the cell. We can explain the data quantitatively using the following minimal set of assumptions.



1. Without any repair mechanism, the cell has a constant, non-zero probability p_{damage} of a lethal event (e.g., DNA damage). From the pure exponential decay of the *lexA3* strain, in which the SOS response is suppressed, we estimated the stochastic death rate due to an unknown damage to be $p_{\text{damage}} = 0.027$ per generation under our experimental conditions.¹ Given

¹ Generation time ~ 21 minutes for cells growing at 37C in Luria-Bertani medium, where cells are exposed to 2 second illumination at every minute with illumination intensity filtered by ND128.

this low probability, we assumed a series of damages occur such that their intervals follow an exponential distribution $e^{-0.027\Delta n}$, where Δn is the number of cell divisions between two consecutive damages. Note that there is a well-defined average timescale for damage, inversely proportional to p_{damage} , $\tau_{\text{break}} = 1/p_{\text{damage}} \sim 37$ divisions (see the red line in **Panel C**).

2. Repair of the unknown damage rate can be modelled as an integrated Gaussian distribution. For example, a small patch of defective cell wall, initially located at the pole because of physical aging of the cell wall component or metabolic inertness, can move to the daughter cell after a certain number of cell divisions because of the growth of the cell wall (see the green line in Panel C). Whatever the source of damage is, our repair

rate function $F(t, \tau_{\text{repair}}, \Delta\tau_{\text{repair}}) = \frac{1}{2} + \frac{1}{2} \operatorname{erf}\left(\frac{t - \tau_{\text{repair}}}{\Delta\tau_{\text{repair}}}\right)$, where erf is the error

function, is characterized by two timescales: the average repair time τ_{repair} and the variation $\Delta\tau_{\text{repair}}$. Note that if $\Delta\tau_{\text{repair}} \sim \tau_{\text{repair}}$, this implies a non-zero basal level of repair activity (Panel B).

3. There is a critical level of accumulated damage, N_{damage^*} , at which the built-in repair mechanism cannot rescue the cell.

Based on this set of assumptions, we have computed the survival and mortality rate curves (black solid lines), where we find the following set of parameters reproduce our data for MG1655 remarkably well: $N_{\text{damage}^*} = 9$ (arbitrary unit); $\tau_{\text{repair}} = 14.5$ generations; $\Delta\tau_{\text{repair}} = 9.5$ generations. Compare these numbers with the average filamentation for every 8.7 divisions.

While our focus has been to explain the mortality data of *E. coli*, our model is general and can help understand the origin of increasing mortality rate (aging). Our key idea is that the timescales underlying the two processes of damage and repair are *comparable* to one another (**Panel C**), and that increasing mortality rate might be a consequence of physical limitation of the repair rate. As a result, the mortality rate will initially be very low, will rise as the fraction of cells with sub-lethal damage rises, but will eventually become constant as the this fraction reaches steady state, thus explicitly recreating the Gompertz curve (Panel B).

In our case, damage (e.g., cell wall defect or aggregation of toxic epigenetic markings) can occur during the repair process (e.g., migration of the defected cell wall or inclusion body to the daughter cell) of the pre-existing damage, and some cells will naturally accumulate the damages beyond the point a built-in repair mechanism can rescue the cell. Accordingly, the mortality rate of the cell also increases with time, although both damage and repair processes have constant

Accompanying note to the complete data sets of Wang et al, Current Biology 20, 1099-1103 (2010).

5

rates and are independent of the replicative age of the cell. For other theories of aging, see, for example, Kirkwood [Cell **120**, 437-447 (2005)].